

## Article

# Apoptosis Induction Associated with Enhanced ER Stress Response and Up-Regulation of c-Jun/p38 MAPK Proteins in Human Cervical Cancer Cells by *Colocasia esculenta* var. *aquaticilis* Hassk Extract

Natharika Chomlamay , Watcharaporn Poorahong , Sukanda Innajak  and Ramida Watanapokasin \* 

Department of Biochemistry, Faculty of Medicine, Srinakharinwirot University, Bangkok 10110, Thailand; natharika.chom@gmail.com (N.C.); noi.poorahong@gmail.com (W.P.); suinnajak@gmail.com (S.I.)

\* Correspondence: ramidabc@gmail.com; Tel.: +66-082-479-7824

**Abstract:** *Colocasia esculenta* var. *Aquaticilis* Hassk, elephant ear (CF-EE) has been widely used as traditional food and medicine. It also shows other therapeutic properties, such as antimicrobial and anti-cancer activity. In this study, we aim to investigate the effect of CF-EE extract on apoptosis induction associated with ER stress in cervical cancer HeLa cells. Cell viability was determined by MTT assay. Assessments of nuclear morphological changes, mitochondrial membrane potential, and intracellular reactive oxygen species (ROS) production were conducted by hoeshst33342, JC-1, and DCFH-DA fluorescence staining, respectively. Sub-G1 DNA content was analyzed by flow cytometry, and protein expression was determined by Western blotting. The results demonstrate that CF-EE extract suppressed HeLa cell growth and induced nuclear condensation and apoptotic bodies. There was also a loss of mitochondrial membrane potential and increased apoptosis marker protein expression, including Bax, cleaved-caspase-7, and cleaved-PARP. In addition, the results show that CF-EE extract induced ROS, increased ER stress proteins (GRP78 and CHOP), enhanced p38 and c-Jun phosphorylation, and inhibited Akt expression in HeLa cells. In summary, CF-EE extract induced apoptotic cell death-associated ROS-induced ER stress and the MAPK/AKT signaling pathway. Therefore, CF-EE extract has anticancer therapeutic potential for cervical cancer treatment in the future.

**Keywords:** *Colocasia esculenta* var. *aquaticilis* Hassk; cervical cancer; endoplasmic reticulum stress; apoptosis; MAPK



**Citation:** Chomlamay, N.; Poorahong, W.; Innajak, S.; Watanapokasin, R. Apoptosis Induction Associated with Enhanced ER Stress Response and Up-Regulation of c-Jun/p38 MAPK Proteins in Human Cervical Cancer Cells by *Colocasia esculenta* var. *aquaticilis* Hassk Extract. *Sci. Pharm.* **2022**, *90*, 45. <https://doi.org/10.3390/scipharm90030045>

Academic Editor: Michael Danilenko

Received: 27 May 2022

Accepted: 7 July 2022

Published: 25 July 2022

**Publisher's Note:** MDPI stays neutral with regard to jurisdictional claims in published maps and institutional affiliations.



**Copyright:** © 2022 by the authors. Licensee MDPI, Basel, Switzerland. This article is an open access article distributed under the terms and conditions of the Creative Commons Attribution (CC BY) license (<https://creativecommons.org/licenses/by/4.0/>).

## 1. Introduction

Cervical cancer is the fourth most common cancer in women worldwide; approximately 604,127 cases and 341,831 deaths were reported in 2020 [1]. The regions with the highest incidence and mortality are Africa, Southeast Asia, and South America [2,3]. The standard treatments of cervical cancer include surgery, radiotherapy, chemotherapy [4], and antibody therapy [5]. However, these treatments have several side effects and drug resistance. Thus, a novel drug and a novel treatment system are urgently needed to possibly increase the survival rate.

*Colocasia esculenta* var. *aquaticilis* Hassk is a plant found in Southeast Asia, specifically in Thailand, China, India, Southern Japan, Northern Australia, and Melanesia [6]. It is commonly known as elephant ear, which is a sub-species of *C. esculenta* in the Araceae family that has widely been used as traditional food and medicine for asthma, arthritis, diarrhea, internal hemorrhage, inflamed glands, neurological disorders, otorrhoea, and skin disorders [7]. Previous studies have shown the major compounds of *C. esculenta* are phenolics and flavonoids [8] including 3,5-di-tert-butyl phenol [9], orientin [10,11], vitexin [11], luteolin-6-C-hexoside-8-C-pentoside, schaftoside, luteolin-3',7-di-O-glucoside, homoorientin, isovitexin, luteolin-40-O-glucoside, luteolin-7-O-glucoside [12], and caffeic acid [13].

Moreover, *C. esculenta* exhibits various biological activities, including analgesic [7], antimicrobial, antifungal [8], anti-diabetic, antihemorrhagic activities [14], anti-inflammation, anthelmintics [15], and anti-cancer [7,14,15].

Endoplasmic reticulum (ER) plays an important role in protein folding and transportation in cells. The dysfunction of ER homeostasis is caused by various stimuli, including calcium imbalance, reactive oxygen species (ROS), and toxic compounds [16]. These factors can induce ER disjunction [17], resulting in the accumulation of un-/misfolded proteins in the lumen of ER, called ER stress. These events require the unfolded protein response (UPR) signaling which readjusts ER folding capacity to restore protein homeostasis [18]. The UPR is stimulated by three transmembrane proteins or ER stress sensors: protein kinase R-like endoplasmic reticulum kinase (PERK), inositol-requiring kinase 1 (IRE1), and activating transcription factor 6 (ATF6). In normal cells, the transmembrane proteins bind to glucose-regulated protein 78 (GRP78) to remain inactive, but when ER stress occurs, these transmembrane proteins dissociate from GRP78, and their dimerization and autophosphorylation lead to their active stage. Activated PERK phosphorylates the  $\alpha$  subunit of eukaryotic initiation factor 2 (eIF2 $\alpha$ ) [19,20] and then activates the nuclear translocation of activating transcription factor 4 (ATF4) into the nucleus. Transcription factor ATF4 induces the transcription of proteins required to restore ER homeostasis, such as ER chaperones proteins and C/EBP homologous proteins (CHOPs) [21]. Prolonged ER stress may cause apoptosis induction via the activities of CHOP protein such as enhances pro-apoptotic proteins [17].

Apoptosis is a programmed cell death that is genetically regulated by a natural process involving various stimuli to destroy cells to maintain cellular homeostasis. It occurs in various processes, such as normal cell turnover and chemical-induced cell death. In addition, this process is used for anti-tumor progression. Apoptotic cells have specific morphological changes, including DNA condensation and apoptotic body formation, induced by caspase activation via different stimuli, such as radiation, toxins, free radicals, viral infections, and ER stress. All these stimuli cause mitochondrial membrane potential changes through pro-apoptotic protein (Bcl-2-associated X—Bax) activation and anti-apoptotic protein (B-cell lymphoma 2—Bcl-2; B-cell lymphoma-extra-large—Bcl-xL; myeloid leukemia 1—Mcl-1) inactivation, which results in caspase activation, PARP inhibition, and cell death [22].

Mitogen-activated protein kinase (MAPK) is a serine-threonine kinase (STKs) related to various cellular mechanisms, including cell survival, proliferation, differentiation, inflammation, and apoptosis [23]. The three subgroups of the MAPK pathway include extracellular signal-regulated kinase (ERK), c-Jun N-terminal kinase (JNK), and p38 kinase [24]. A previous study reported that ERK1/2 activation promoted cell survival through the induction of anti-apoptotic proteins, such as Bcl-2, Mcl-1, and Bcl-xL [25]. Meanwhile, both JNK and p38 MAPK are related to cell death via p53 phosphorylation, caspase-8 activation, and anti-apoptotic protein Bcl-2 inhibition [26]. However, the role of CF-EE extract-induced apoptosis via ER stress response in human cervical cancer has not been reported. Therefore, in this study, we aimed to show that CF-EE extract can induce apoptosis associated with ER stress, MAPK, and Akt signaling pathway in cervical cancer HeLa cells.

## 2. Materials and Methods

### 2.1. Reagents

Dulbecco's modified Eagle medium (DMEM), fetal bovine serum (FBS), penicillin streptomycin, and trypsin-EDTA were purchased from HIMEDIA (HiMedia, Laboratories, Mumbai, India). 3-(4,5-dimethylthiazol-2-yl)-2,5-diphenyltetrazolium bromide (MTT) and dimethyl sulfoxide (DMSO) were purchased from Sigma-Aldrich (St. Louis, MO, USA). 2'-(4-Ethoxyphenyl)-6-(4-methyl-1-piperazinyl)-1H,3'H-2,5'-bibenzimidazole (Hoechst 33342) was purchased from Thermo Fisher Scientific, Inc. (Invitrogen™, Waltham, MA, USA). 5,5',6,6'-Tetrachloro-1,1',3,3-tetraethylbenzimidazolylcarbocyanine iodide (JC-1) was purchased from Sigma-Aldrich (Merck KGaA, Darmstadt, Germany). Bovine serum albumin (BSA) was purchased from VWR (VWR International Ltd., PA, USA). Guava Cell Cycle® reagent,

dichlorodihydrofluorescein diacetate (DCFH-DA) fluorescence dye, phenylmethylsulfonyl fluoride (PMSF), and antibody against  $\beta$ -actin were purchased from Merck Millipore (Merck KGaA, Darmstadt, Germany). For immunoblotting analysis, antibodies against GRP78, calnexin, PARP, caspase-7, p38, p-p38 at Thr180/Tyr182, c-Jun, p-c-Jun at Thr183/Tyr185, p44/42 MARP (ERK1/2), p-p44/42 MARP (ERK1/2) at Thr202/Tyr204, Bcl-2, Bcl-xL, Bax, Mcl-1, p-PDK1, p-Akt at Ser473, Akt, anti-mouse immunoglobulin G, and anti-rabbit immunoglobulin G horseradish peroxidase conjugated secondary antibodies were purchased from Cell Signaling Technology (Danvers, MA, USA).

## 2.2. Plant Extraction and Identification

The fresh stem of *Colocasia esculenta* var. *aquatilis* Hassk, known as elephant ear (CF-EE) was harvested from Chiang Mai in October 2020 for crude extract preparation. Briefly, fresh CF-EE stems were cut and dried at 50 °C for 5 days. After that, the dry samples were ground and soaked in 50% acetone (5% *w/v*) (Jakraval Application Co., Ltd, Nonthaburi, Thailand). Then, the mixture was filtered through a Whatman No.4 filter paper and evaporated. In the next step, the water part was fractionated by partition with ethyl acetate at a ratio of 1:1 (V/V) in a separating funnel. The ethyl acetate part (upper) was then collected and evaporated. The crude CF-EE extract was dissolved in dimethyl sulfoxide (DMSO) before the experiments. The caffeic acid content in the CF-EE extract was identified by Agilent 1200 series high-performance liquid chromatography (HPLC) system (Agilent Technologies, Inc., CA, USA) at room temperature. The column was Zorbax Eclipse XDB-C18 (4.6×150 mm, 5 micro) (Merck KGaA, Darmstadt, Germany). The mobile phase was 2% acetic acid in water (gradient) at a flow rate of 0.6 mL/min. The UV detection wavelength was set at 327 nm. A compound of the crude extract was identified as caffeic acid.

## 2.3. Cell Lines and Cell Culture

Cervical cancer HeLa cells were purchased from American Type Culture Collection (ATCC, Manassas, VA, USA). The cells were cultured with Dulbecco's modified Eagle medium (DMEM) supplemented with 10% fetal bovine serum, penicillin (100 IU/ml), and streptomycin (100 µg/mL) at 37 °C in a humidified atmosphere of 5% CO<sub>2</sub>. The cells were sub-cultured by 0.25% trypsin-EDTA at 80% confluence every 2–3 days.

## 2.4. Cytotoxicity Assay

MTT assay was used to determine the cell viability of the HeLa cells. The cells were seeded at  $0.7 \times 10^4$  cells/well and incubated overnight. They were then treated with CF-EE extract at concentrations of 0, 25, 50, 100, 200, 300, and 400 µg/mL for 24 h. The cells were replaced with 0.5 mg/mL of MTT solution at 37 °C for 2 h. The formazan crystal was dissolved by DMSO. The optical density at 570 nm was measured using a microplate reader (Multiskan Sky Microplate Spectrophotometer, Waltham, MA, USA). All experiments were conducted in three independent replicates. The cell viability and half-maximal inhibitory concentration (IC<sub>50</sub>) values were calculated using the GraphPad Prism 9 software (GraphPad Prism Software, Inc., San Diego, CA, USA).

## 2.5. Detection of Nuclear Morphological Changes

The determination of nuclear change was performed following the methods of Yangnok K et al. [27]. Briefly, HeLa cells were seeded at  $6 \times 10^4$  cells/well and incubated overnight. The cells were treated with 100, 150, 200, 250, and 300 µg/mL of CF-EE extract for 6 h, and subsequently stained with 5 µg/mL Hoechst 33342 for 30 min. They were then observed using a fluorescence microscope at 20× magnification (IX71 Olympus, Tokyo, Japan).

### 2.6. Mitochondrial Membrane Potential ( $\Delta\Psi_m$ ) Detection

HeLa cells were seeded at  $6 \times 10^4$  cells/well and incubated overnight. The cells were treated with CF-EE extract at various concentrations for 6 h, and then stained with  $5 \mu\text{g/mL}$  of 5,5',6,6'-tetrachloro-1,1',3,3'-tetraethyl benzimidazol carbocyanine iodide (JC-1) dye for 10 min. Then, the cells were observed under a fluorescence microscope at  $20\times$  magnification (IX71 Olympus, Tokyo, Japan).

### 2.7. Cell Cycle Analysis

A cell cycle analysis assay was performed following the method of Yangnok K, et al. [27]. Briefly, HeLa cells were seeded at  $10^5$  cells/well and incubated overnight. The cells were treated with CF-EE extract at various concentrations for 12 h, then fixed with 70% cold ethanol and stained according to the manufacturer's instructions (Guava Cell Cycle<sup>®</sup> reagent from Merck KGaA). The cells were analyzed for DNA content using the Guava easyCyte<sup>™</sup> flow cytometer and GuavaSoft<sup>™</sup> software (Merck Millipore Corporation, Merck KGaA, Darmstadt, Germany).

### 2.8. Detection of Intracellular ROS

HeLa cells were seeded at  $6 \times 10^4$  cells/well and incubated overnight. The cells were treated with CF-EE extract at various concentrations for 3 h, then stained with  $20 \mu\text{M}$  of dichlorodihydrofluorescein diacetate (DCFH-DA) fluorescence dye and incubated at  $37^\circ\text{C}$  for 30 min. Then, the cells were observed under a fluorescence microscope at  $20\times$  magnification (IX71 Olympus, Japan).

### 2.9. Western Blot Analysis

After 24 h of treatment, the cells were harvested and lysed in RIPA buffer (50 mM Tris, pH 7.5, 5 mM EDTA, 250 mM NaCl, 0.5% TritonX-100, protein inhibitor tablet) (Roche Diagnostics GmbH, Mannheim, Germany). Using 8–12% of SDS-PAGE,  $20 \mu\text{g}$  of each protein sample was resolved and transferred onto polyvinylidene fluoride (PVDF) membranes. The membrane was blocked with 5% non-fat milk powder (*w/v*) and then incubated with antibodies against CHOP and rabbit monoclonal antibody against GRP78, calnexin, PARP, caspase-7, p38, p-p38 at Thr180/Tyr182, c-Jun, p-c-Jun at Thr183/Tyr185, p44/42 MAPK (ERK1/2), p-p44/42 MAPK (ERK1/2) at Thr202/Tyr204, Bcl-2, Bcl-xL, Bax, Mcl-1, p-PDK1, p-Akt at Ser473, Akt, and  $\beta$ -actin (1:1000) at  $4^\circ\text{C}$  overnight. This was followed by incubation with horseradish peroxidase (HRP) conjugated secondary antibody for 1 h. The protein expression was amplified using Immobilon<sup>™</sup> Western chemiluminescent HRP substrate solution (Merck KGaA, Darmstadt, Germany) and detected using gel documentary machine (AllianceQ9 advanced, Cambridge, UK).

### 2.10. Statistical Analysis

The results are presented as the mean  $\pm$  standard deviation (SD) obtained from the three independent experiments ( $n = 3$ ). Using SPSS statistical software version 25 (IBM Corp., NY, USA), the treatment groups were assessed by one-way analysis of variance (one-way ANOVA) using Tukey's post hoc test, and *p*-values of 0.05 ( $p < 0.05$ ) and 0.01 ( $p < 0.01$ ) were considered statistically significant.

## 3. Results

### 3.1. HPLC Analysis of Caffeic Acid

Chromatography HPLC analysis was carried out on a Zorbax Eclipse XDB-C18 ( $4.6 \times 150 \text{ mm}$ ,  $5 \mu\text{m}$ ) chromatographic column at room temperature to identify the crude CF-EE extract by comparing it to a standard. The mobile phase was 2% acetic acid in water at a flow rate of  $0.6 \text{ mL/min}$ , and the injection volume was  $20 \mu\text{L}$ . The UV detection wavelength was set at  $327 \text{ nm}$ . The standard curve of caffeic acid was retention time ( $R_t$ ) =  $8.420 \text{ min}$ , as shown in Figure 1A. The chromatographic HPLC characterization revealed the presence of a peak with  $R_t$  at  $8.434 \text{ min}$ . The results demonstrate that EE

extract exhibited a peak at the same  $R_t$  of standard caffeic acid (Figure 1B). These results indicate the CF-EE extract consist of caffeic acid content. However, the other components of CF-EE extract require further investigation.

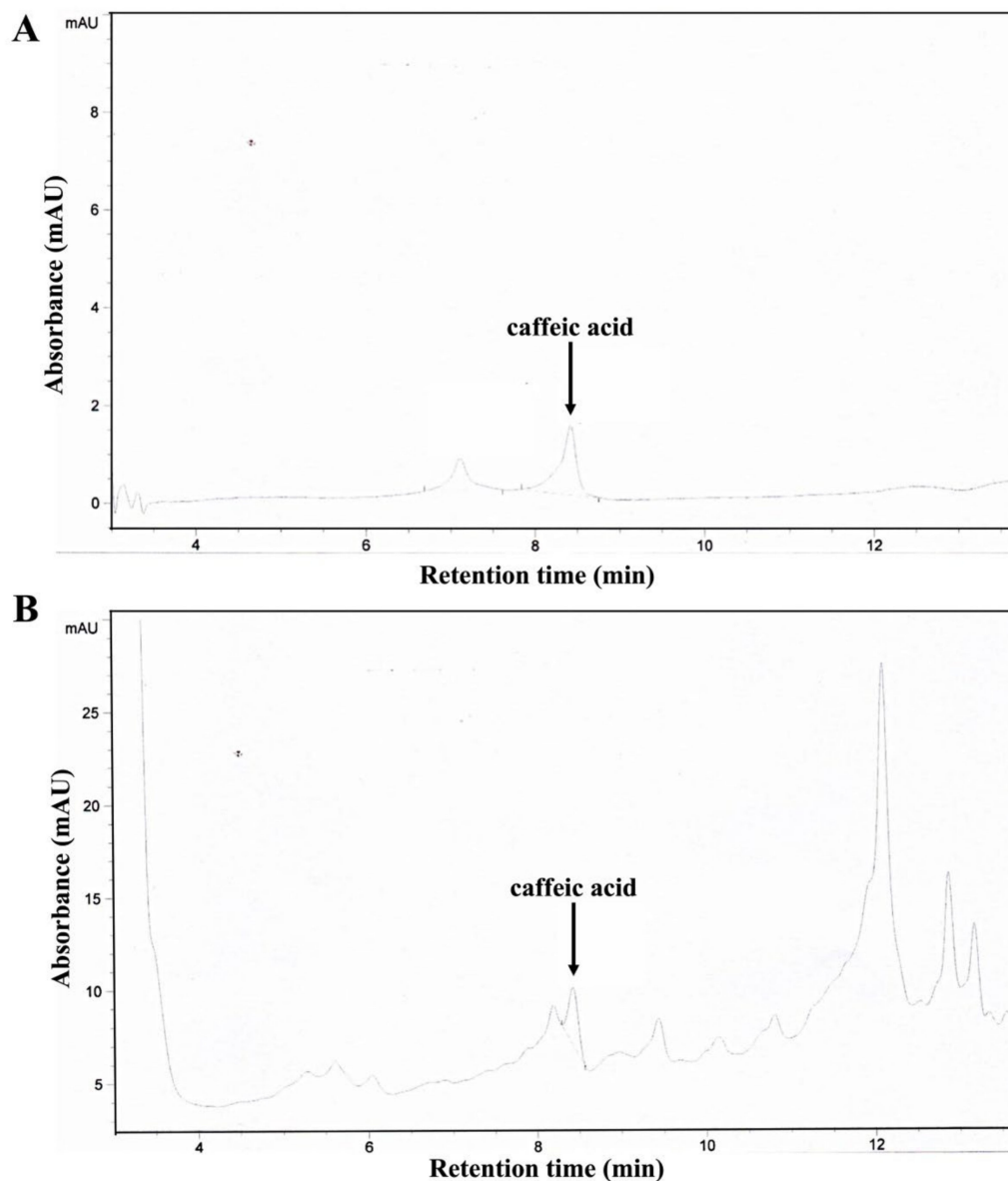


**Figure 1.** HPLC chromatograms of (A) caffeic acid standard ( $R_t = 8.420$  min) and (B) CF-EE extract chromatographic condition; Zorbax Eclipse XDB-C18 column ( $4.6 \times 150$  mm, 5 micro). Mobile phase: 2% acetic acid–water (gradient) at a flow rate of 0.6 mL/min; UV detection wavelength: 327 nm.

### 3.2. CF-EE Suppresses Cell Proliferation of HeLa Cells

MTT assay was performed to investigate the cytotoxic effect of CF-EE extract on cervical HeLa cells. We found that 24 h treatment of CF-EE extract significantly decreased HeLa cell viability in a dose-dependent manner with  $187.2 \pm 0.34$   $\mu\text{g}/\text{mL}$  of  $\text{IC}_{50}$  (Figure 2).

### 3.3. Effect of CF-EE Extract on Apoptosis Induction in HeLa Cells

The nuclear morphological changes in HeLa cells were determined by Hoechst 33342 staining. Our results show that CF-EE extract increased nuclear condensed cells and apoptotic bodies in a dose-dependent manner when compared to the control group (Figure 3A,C). Additionally, the results of the mitochondrial membrane potential detection show that CF-EE extract induced mitochondrial depolarization by a significantly decreased relative red

fluorescence intensity in a dose-dependent manner when compared to the control group (Figure 3B,D).

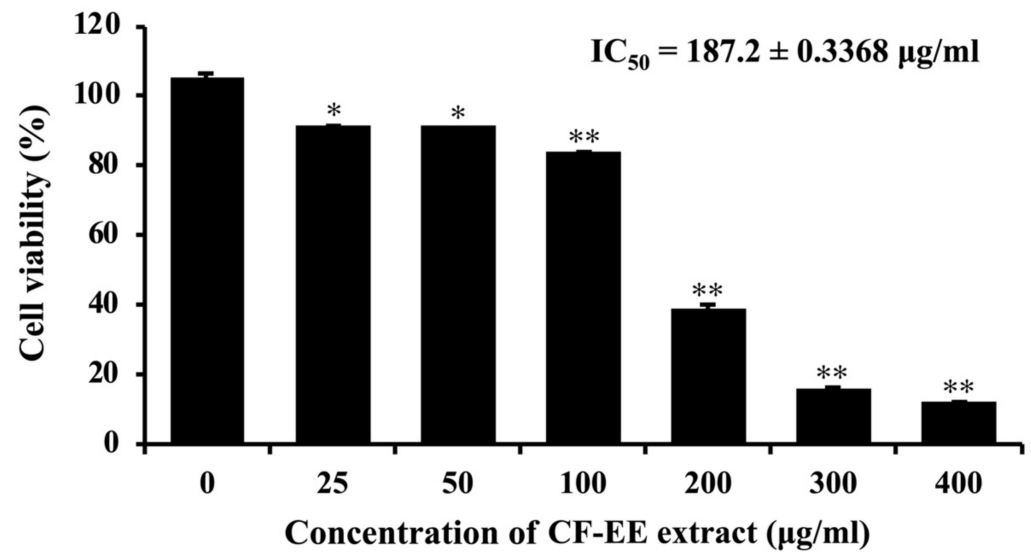


**Figure 2.** CF-EE extract inhibited cell growth in HeLa cells. The cells were treated with CF-EE extract at various concentrations for 24 h and MTT assay was performed. The  $IC_{50}$  of the CF-EE extract was  $187.2 \pm 0.3386 \mu\text{g/mL}$ . \*  $p < 0.05$  and \*\*  $p < 0.01$  compared with the control.

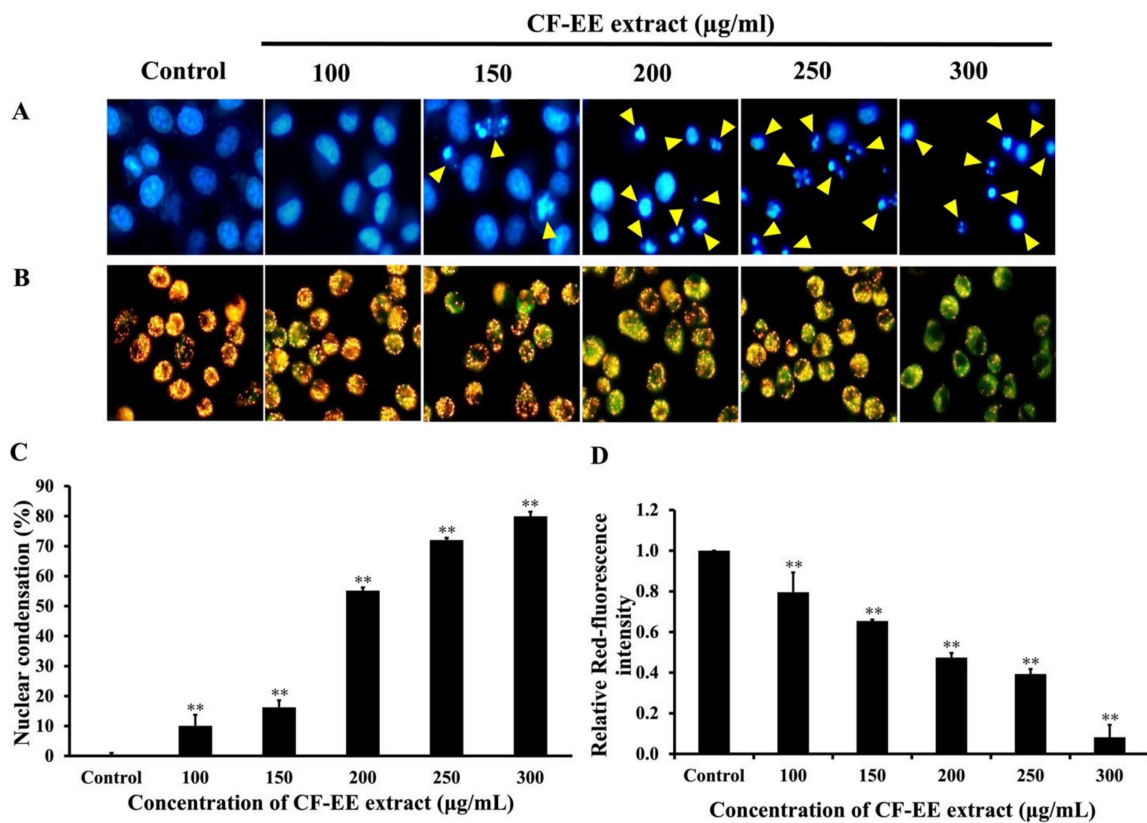


**Figure 3.** Effect of CF-EE extract on apoptosis induction in HeLa cells. (A) Nuclear morphological changes after Hoechst33342 staining observed by fluorescence microscopy (20X). Yellow arrow indicates nuclear condensed cells and apoptotic bodies. (B) Loss of mitochondrial membrane potential in CF-EE extract-treated cells observed by fluorescence microscopy (20X). (C) Percentage of nuclear condensation compared to the control. (D) Relative red-fluorescence intensity compared to the control. The values are represented as the mean  $\pm$  SD. \*\*  $p < 0.01$  compared to the control.

### 3.4. CF-EE Extract Induces Sub-G1 Population in HeLa Cells

To clarify whether CF-EE extract could induce apoptosis in HeLa cells, we investigated the sub-G1 DNA content using flow cytometry. The results show that CF-EE extract increased the sub-G1 population from 1.29, 1.38, 4.42, 8.74, and 12.42% at 100, 150, 200, 250, and 300 µg/mL of CF-EE extract, respectively, compared to the control group (1.17%) (see Figure 4A). These results demonstrate that CF-EE extract showed a potential anti-cancer effect through apoptosis induction in HeLa cells.

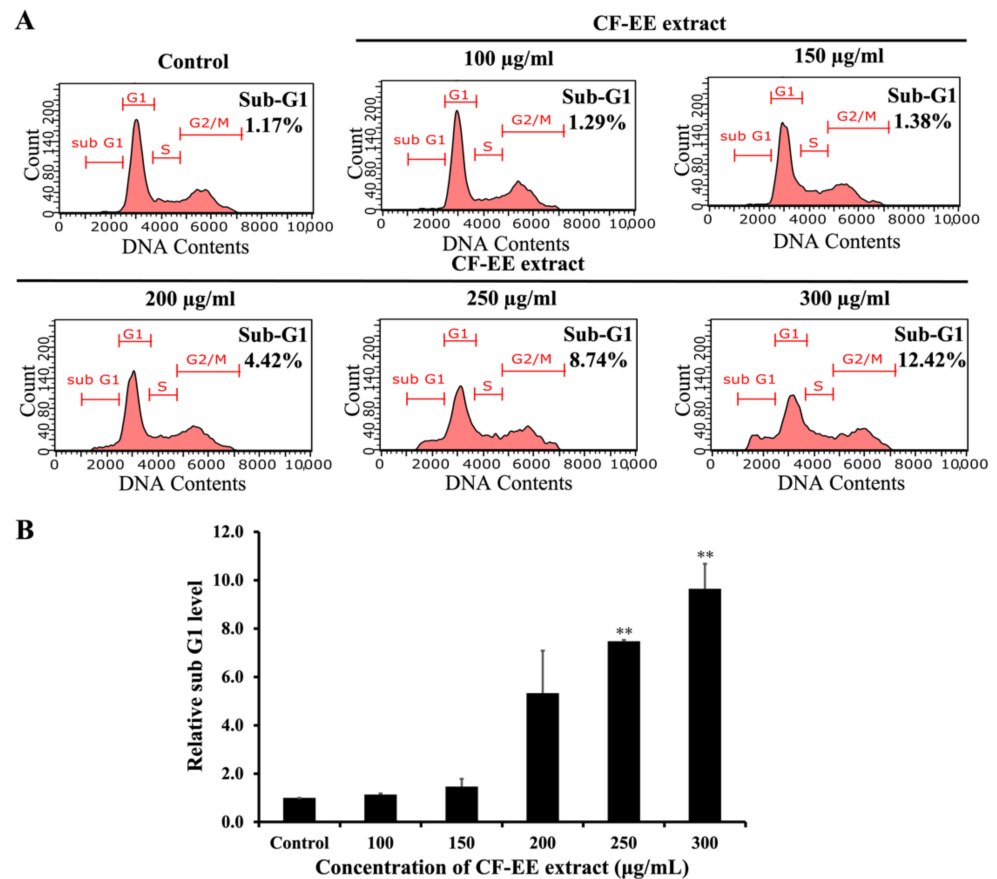


**Figure 4.** Effect of CF-EE extract on the accumulation of sub-G1 population in HeLa cells. The cells were treated with 100, 150, 200, 250, and 300 µg/mL of CF-EE extract for 12 h. The cells were fixed and stained with Guava Cell Cycle<sup>®</sup> reagent, then analyzed by a flow cytometer. (A) DNA content profiles. (B) Relative sub-G1 level of CF-EE extract-treated cells. The values are represented as the mean ± SD. \*\*  $p < 0.01$  compared to the control.

### 3.5. CF-EE Extract Induces Oxidative Stress in HeLa Cells

Previous data have demonstrated that CF-EE extract induced the loss of mitochondrial potential, causing an intrinsic apoptotic pathway. It is well-known that oxidative stress predominantly induces this event. Therefore, we examined intracellular reactive oxygen species (ROS) production in HeLa cells using DCFH-DA staining and fluorescence microscopy. The results show that CF-EE extract significantly increased ROS generation in CF-EE extract-treated cells compared to the control group, as shown in Figure 5.

### 3.6. CF-EE Extract Induces Endoplasmic Reticulum Stress in HeLa Cells

Oxidative stress is one of the factors that induce ER stress. Our results show that CF-EE extract induced the accumulation of intracellular ROS in the cells. Therefore, the ER stress responses in the CF-EE-treated cells were investigated by comparing them to cells treated with tunicamycin, an ER stress inducer. The results show that CF-EE extract significantly decreased calnexin in CF-EE-treated cells at  $p < 0.05$  compared to the control

group. Meanwhile, the expressions of GRP78 and CHOP were increased in CF-EE-treated cells correlated with the Tm-treated cells (Figure 6). Remarkably, the results demonstrate that CF-EE extract mainly increased CHOP levels in HeLa cells. Thus, we hypothesize that CF-EE extract induced ER stress, triggering apoptosis in HeLa cells.

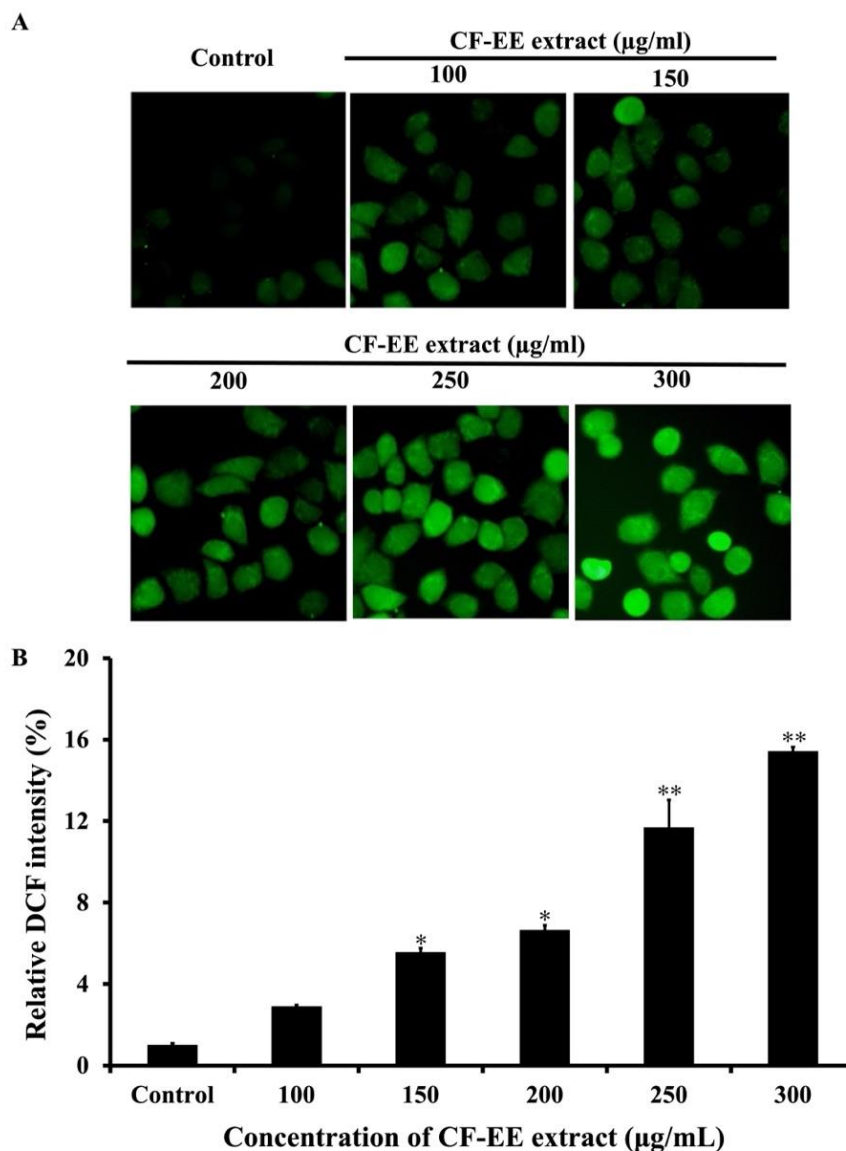


**Figure 5.** Effect of CF-EE extract on intracellular ROS production in HeLa cells. The cells were stained with 20 µM of DCFH-DA and visualized by a fluorescence microscope (20×). (A) DCF-fluorescence signal (green-color) in cells, observed under a fluorescence microscope. (B) The average relative DCF-fluorescence intensity. \*  $p < 0.05$  and \*\*  $p < 0.01$  compared to the control.

### 3.7. CF-EE Extract Activates Intrinsic Apoptotic Pathway in HeLa Cells

To confirm the effect of CF-EE extract on the ER stress-associated intrinsic apoptosis on HeLa cells, we investigated the apoptosis marker proteins and compared them to the Tm group by Western blot analysis. The results demonstrate that CF-EE extract decreased the expression of anti-apoptotic proteins (Bcl-2, Mcl-1, and Bcl-xL) in a dose-dependent manner and increased pro-apoptotic proteins (Bax) as shown in Figure 7A,B. In addition, increased cleaved-caspase-7 and cleaved-PARP expression was also detected, correlating with the Tm-treated group (Figure 7A,C).



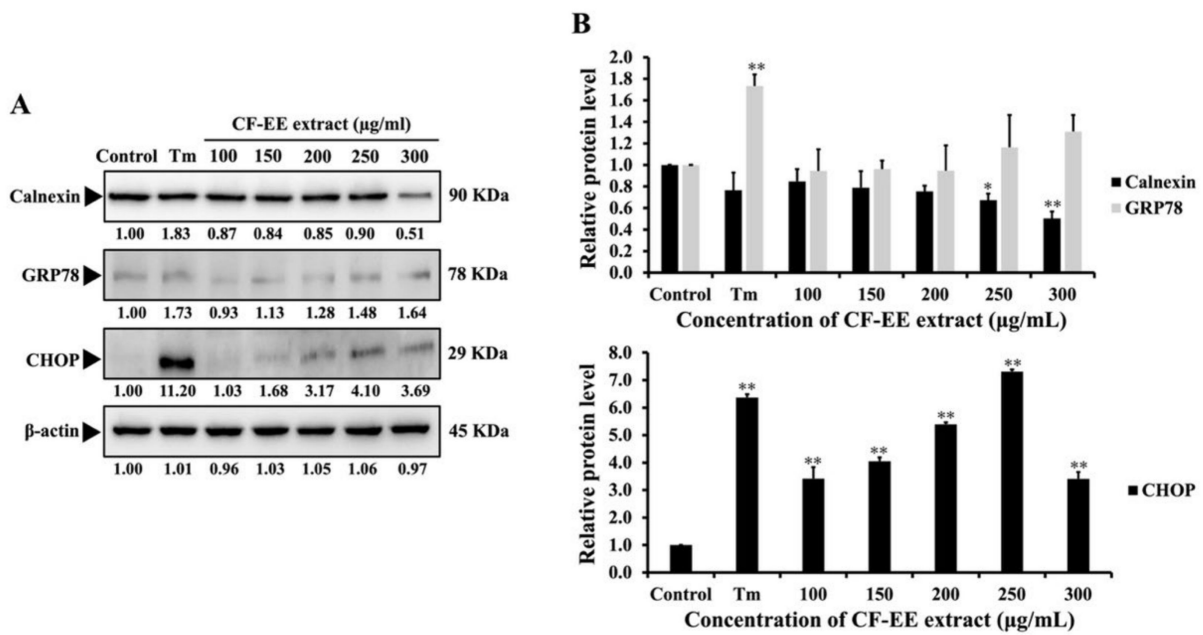


**Figure 6.** CF-EE extract induced ER stress signaling pathway. HeLa cells were treated with CF-EE extract at various concentrations or 10 µg/mL of Tm for 24 h. (A) Expressions of calnexin, GRP78, and CHOP were determined by Western blotting. (B) Relative protein intensity compared to the control, β-actin, was used as an internal control. The values are represented as the mean ± SD. \*  $p < 0.05$  and \*\*  $p < 0.01$  compared to the control.

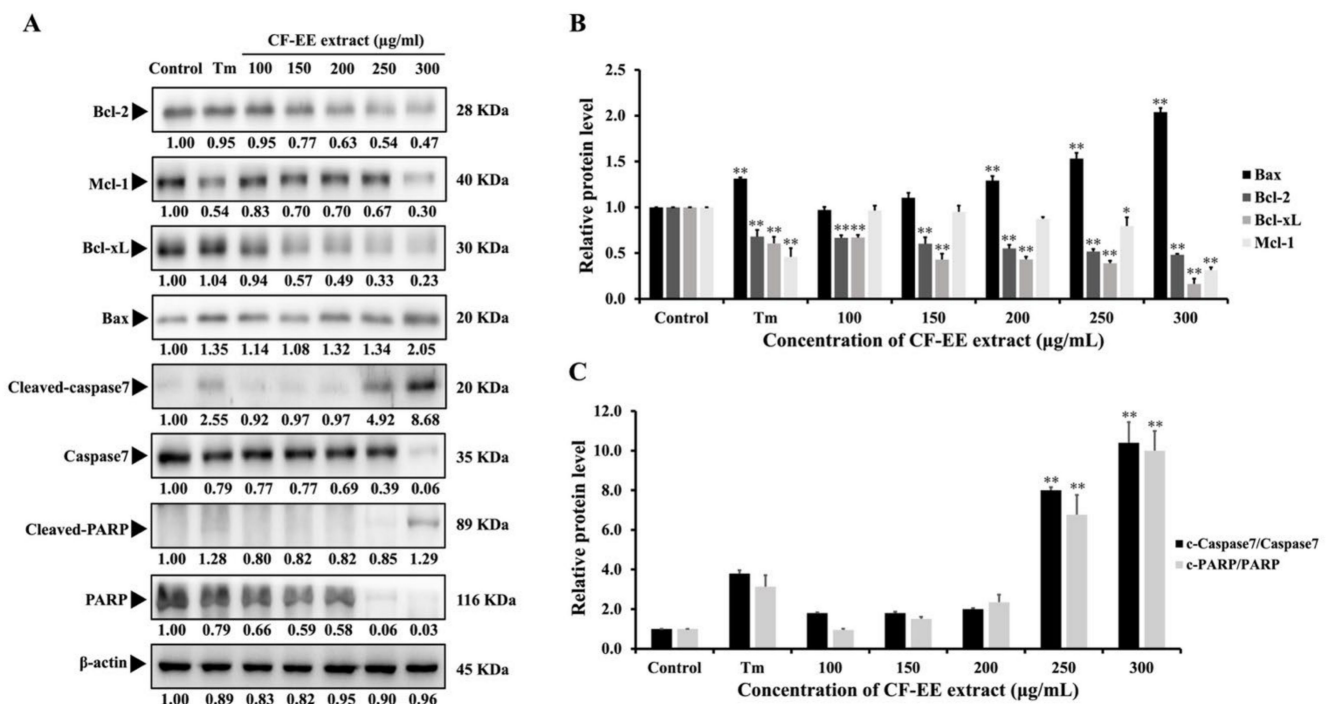


**Figure 7.** Effect of CF-EE extract on apoptosis pathway in HeLa cells. The cells were treated with CF-EE extract at various concentrations or 10 µg/mL of Tm for 24 h. The protein expressions were investigated by Western blotting. (A) Decreased Bcl-2, Bcl-xL, Mcl-1, and increased Bax, cleaved-caspase-7/caspase-7, and cleaved-PARP/PARP were detected. (B,C) Relative protein band intensity, β-actin was used as an internal control. The values are represented as the mean ± SD. \*  $p < 0.05$  and \*\*  $p < 0.01$  compared to the control.

### 3.8. Effect of CF-EE Extract on MAPK and Akt Signaling Pathway in HeLa Cells

To examine the effect of CF-EE extract on MAPK and the Akt signaling pathway in HeLa cells, Western blot analysis was conducted. Our results show that CF-EE extract significantly increased the ratio between the phosphor-form and total-form of MAPK proteins, including p-p38/p38, p-c-Jun/c-Jun, and significantly decreased p-ERK1/2/ERK1/2 in a dose-dependent manner in CF-EE-treated cells (Figure 8A,B). Meanwhile, the protein levels of p-PDK1, Akt, and p-Akt (Ser473) were decreased in CF-EE-treated cells at  $p$ -value < 0.01 compared to the control group, as shown in Figure 8C,D. These results indicate that CF-EE extract may inhibit cervical cancer HeLa cell growth by activating MAPKs and suppressing Akt activities in HeLa cells.

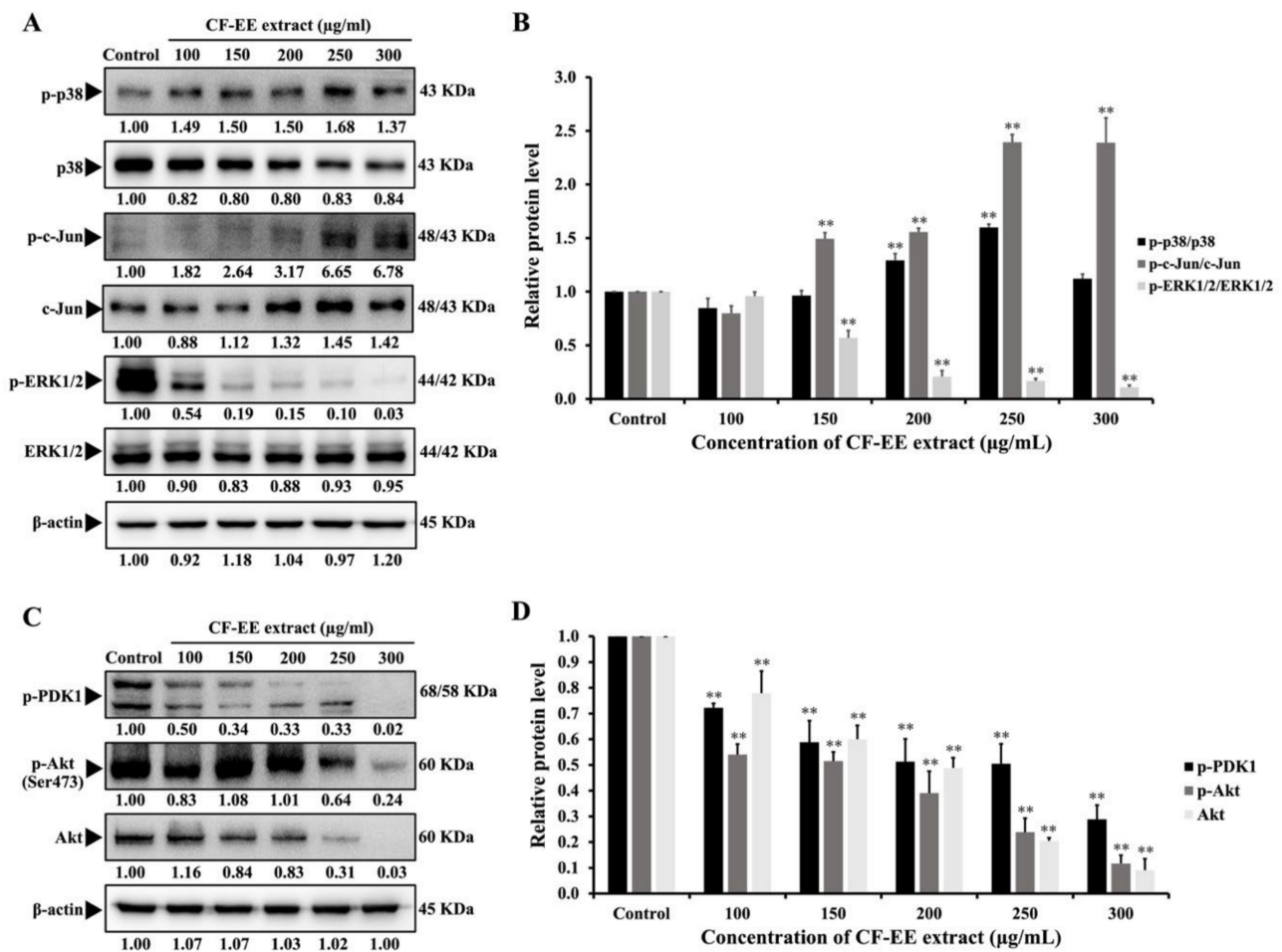


**Figure 8.** Effect of CF-EE extract on MAPK and Akt pathway. HeLa cells were treated with CF-EE extract at various concentrations for 24 h, and protein expression was determined by Western blot analysis. (A) Expression of p-p38, p38, p-c-Jun, c-Jun, p-ERK1/2, and ERK1/2. (B) Relative band intensity of MAPKs protein. (C) Expression of p-PDK1, Akt, and p-Akt(Ser473). (D) Relative band intensity of p-PDK1, Akt, and p-Akt(Ser473).  $\beta$ -actin was used as an internal control. The values are represented as the mean  $\pm$  SD. \*\*  $p$  < 0.01 compared to the control.

### 4. Discussion

CF-EE extract was isolated from the stem of *C. esculenta* var. *aquatilis* Hassk from the northern part of Thailand. Previous study has shown that compounds of *C. esculenta* are phenolic and flavonoid [8]. The crude extract of *C. esculenta* consists of flavonoids, which are of great interest in the pharmaceutical industry. Flavonoids were shown to have antioxidant [28] and anti-tumor properties in cancer cells [29]. Our study found that a compound of EE extract is caffeic acid (Figure 1), which was determined by HPLC

system. Caffeic acid (3,4-dihydroxycinnamic) is a phenolic compound distributed in plants including coffee, berries, carrot, honey, potatoes, and herbs [30]. Previous studies have demonstrated that caffeic acid has many pharmacological properties including antimicrobial [31], anti-inflammatory [32], immunomodulatory activity [33], anti-proliferation, and anti-cancer [34]. This compound is a ROS-scavenging agent in normal cells, but it is cytotoxic to cancer cells [35]. Kanimozhi et al. showed the anti-tumor effect of caffeic acid in cervical cancer HeLa cells and human fibrosarcoma ME-180 cells [36]. Consistent with this result, we found that CF-EE extract inhibited HeLa cell growth with concentrations ranging from 100 to 300 µg/mL in a dose-dependent manner.

Apoptosis is the process of programmed cell death, which plays an important role in cancer cell death [37]. The remarkable morphological characteristics of apoptosis are chromatin condensation, nuclear fragmentation, membrane blebbing, and apoptotic bodies [38]. Our results demonstrate that CF-EE extract increased nuclear fragmentation and apoptotic bodies in a dose-dependent manner. Moreover, we found that CF-EE extract also induced the dysfunction of mitochondria by disrupting their potential leading to the intrinsic apoptotic pathway. Therefore, we hypothesized that CF-EE extract might induce apoptosis in HeLa cells, which we confirmed by investigating the sub-G1 content in HeLa-treated cells. The results confirmed that CF-EE extract has the potential to induce apoptosis in HeLa cells. In fact, the intrinsic apoptotic pathway is mainly promoted by the accumulation of intracellular ROS. Our results show that CF-EE extract also promoted intracellular ROS production in HeLa cells.

It is well-known that oxidative stress is the cause of cellular organelle damage, including ER. A previous study demonstrated that increasing ROS led to ER stress induction [39]. Therefore, we investigated the expressions of proteins related to ER stress and apoptosis induction. ER stress is a condition of un-/misfolded protein accumulation. This event leads to the activation of transmembrane protein responses to ER stress including PERK, IRE1, and ATP6. Prolonged ER stress causes CHOP-induced apoptosis in cells. This mechanism is stimulated via PERK/eIf2 $\alpha$ /ATF4/CHOP signaling pathway [40,41]. Many reports have shown that ER stress could activate apoptosis in various cancer cells. Importantly, CHOP is a critical pro-apoptosis transcription factor that regulates the expression of Bcl-2 family proteins [42]. Notably, previous evidence has shown that CHOP decreased the expression of anti-apoptotic proteins (Bcl-2 and Bcl-xL) but increased the expression of pro-apoptotic proteins (Bim, Puma, Noxa, Bak, and Bax) [19]. Previous study demonstrated that ER stress mediated apoptosis induction in human breast cancer MCF-7 cells [43]. Our studies found that the expression of GRP78 and CHOP was increased which correlated with the increased pro-apoptotic proteins and decreased anti-apoptotic proteins, resulting in apoptosis induction in HeLa cells after CF-EE extract treatment. The results indicated that CF-EE extract enhanced CHOP level which could lead to the intrinsic apoptosis induction and disturbance of the balance between pro- and anti-apoptotic proteins, causing the mitochondrial apoptotic pathway. These events lead to caspase and apoptosis induction. We found that CF-EE extract increased effector caspase-7 activity and induced PARP cleavage, resulting in apoptosis in HeLa cells. These results correlate with several studies showing that cleaved caspase-3 and -7 promote DNA fragmentation, nuclear condensation, and PARP inhibition, resulting in apoptosis [44–46]. Interestingly, previous studies have reported that caffeic acid also acted as a pro-oxidant and enhanced ROS generation in HeLa and H180 cancer cells [34,36]. Likewise, caffeic acid from *Ocimum gratissimum* Linn induced apoptosis in HeLa cells by increasing nuclear fragmentation, cleaved caspase-3, and p53 expression [47]. Based on these data, CF-EE extract induced ER stress-associated apoptosis in HeLa cells. However, for a better understanding, the deep mechanism between ER stress and apoptosis induction by CF-EE extract requires further investigation.

Previous studies have shown that MAPK signaling pathway is an important signaling pathway that activates apoptosis [18,25]. Lee et al. reported that caffeic acid induced cell death by enhancing p-JNK1 and p-p38 in rat C6 glioma cells [48], whereas both p-JNK and p-p38 could phosphorylate Mcl-1 at Ser121 and Thr163 [49]. In addition, JNK inactivates

Bcl-2 [50] and activates Bim [51,52]. JNK-blocked cells did not show apoptosis [53]. Similarly, p-p38 induced apoptosis through Bim activation and Bcl-2 inactivation [52]. While our results demonstrated that CF-EE extract increased the expression of p-p38 and p-c-Jun in HeLa cells. On the contrary, the expression of ERK1/2 was decreased in CF-EE extract-treated cells. Our results indicated that CF-EE extract induced apoptosis associated with MAPK signaling pathway. In addition, Akt signaling pathway plays important roles in cell survival and suppresses apoptosis. In human prostate cancer cells (LNCaP, DU-145, and PC-3), the inhibition of Akt signaling pathway promotes apoptotic cells [54]. Inactivated Akt induces Bad activation [55]. Our results showed that CF-EE extract inhibited p-PDK1 and p-Akt (Ser473), suggesting that CF-EE extract induced apoptosis, associated with ER stress, activated MAPK proteins, and suppressed Akt protein levels in HeLa cells.

## 5. Conclusions

In conclusion, our results demonstrate that CF-EE extract induced the intrinsic apoptotic pathway associated with ER stress in cervical cancer HeLa cells indicated by reduced anti-apoptotic proteins, increased pro-apoptotic proteins, and caspase-7 activation. Moreover, CF-EE extract enhanced p-c-Jun and p-p38 and attenuated ERK1/2 phosphorylation in HeLa cells, as well as inhibited Akt signaling pathway. Thus, CF-EE extract has potential as an anti-cancer therapeutic drug for cervical cancer treatment and should be further studied in depth in the future.

**Author Contributions:** N.C.—investigation and writing of original draft. W.P.—reviewed and edited manuscript. S.I.—planned the experiments. R.W.—supervised, acquired funding, planned the experiments, revised and approved the final manuscript. All authors have read and agreed to the published version of the manuscript.

**Funding:** This study was supported by the Strategic Wisdom and Research Institute, Srinakharinwirot University, Thailand. Grant number 013/2564.

**Institutional Review Board Statement:** Not applicable.

**Informed Consent Statement:** Not applicable.

**Data Availability Statement:** The datasets analyzed during the current study are available from the corresponding author upon reasonable request.

**Acknowledgments:** We thank the Graduate School of Srinakharinwirot University and the Faculty of Medicine, Srinakharinwirot University, Bangkok, Thailand for the materials, instruments, and laboratory rooms.

**Conflicts of Interest:** The authors declare that there is no conflict of interest regarding the publication of this article.

## References

1. Ferlay, J.; Colombet, M.; Soerjomataram, I.; Parkin, D.M.; Piñeros, M.; Znaor, A. Cancer statistics for the year 2020: An overview. *Int. J. Cancer* **2021**, *149*, 1–12. [[CrossRef](#)] [[PubMed](#)]
2. Sung, H.; Ferlay, J.; Siegel, R.L.; Laversanne, M.; Soerjomataram, I.; Jemal, A. Global Cancer Statistics 2020: GLOBOCAN Estimates of Incidence and Mortality Worldwide for 36 Cancers in 185 Countries. *CA Cancer J. Clin.* **2021**, *71*, 209–249. [[CrossRef](#)] [[PubMed](#)]
3. Cao, W.; Chen, H.D.; Yu, Y.; Li, N.; Chen, W. Changing profiles of cancer burden worldwide and in China: A secondary analysis of the global cancer statistics 2020. *Chin. Med. J.* **2021**, *137*, 783–791. [[CrossRef](#)] [[PubMed](#)]
4. Hrgovic, Z.; Fures, R.; Stanic, Z. The diagnostics and treatment of cervical cancer. *Acta. Med. Croatica* **2021**, *75*, 53–68.
5. Park, S.; Kim, M.; Lee, S.; Jung, W.; Kim, B. Therapeutic Potential of Natural Products in Treatment of Cervical Cancer: A Review. *Nutrients* **2021**, *13*, 154. [[CrossRef](#)]
6. Ahmed, I.; Lockhart, P.J.; Ago, E.; Naing, K.W.; Nguyen, D.V.; Medhi, D.K. Evolutionary origins of taro (*Colocasia esculenta*) in Southeast Asia. *Ecol. Evol.* **2020**, *10*, 13530–13543. [[CrossRef](#)]
7. Prajapati, R.; Kalariya, M.; Umbarkar, R.; Parmar, S.; Sheth, N. *Colocasia esculenta*: A potent indigenous plant. *Int. J. Nutr. Pharmacol. Nephrol. Dis.* **2011**, *1*, 90–96. [[CrossRef](#)]
8. El-Mesallamy, A.M.; El-Tawilb, N.A.; Ibrahim, S.A.; Hussein, S.A. Phenolic Profile: Antimicrobial Activity and Antioxidant Capacity of *Colocasia esculenta* (L.) Schott. *Egypt. J. Chem.* **2021**, *64*, 2165–2172.

9. Eleazu, C.O. Characterization of the natural products in cocoyam (*Colocasia esculenta*) using GC–MS. *Pharm Biol.* **2016**, *54*, 2880–2885. [[CrossRef](#)]
10. Pawar, H.A.; Choudhary, P.D.; Kamat, S.R. An Overview of Traditionally Used Herb, *Colocasia esculenta*, as a Phytomedicine. *Med. Aromat. Plants* **2018**, *7*, 1000317. [[CrossRef](#)]
11. Li, H.M.; Hwang, S.H.; Kang, B.G.; Hong, J.S.; Lim, S.S. Inhibitory Effects of *Colocasia esculenta* (L.) Schott Constituents on Aldose Reductase. *Molecules* **2014**, *19*, 13212–13224. [[CrossRef](#)]
12. Lebot, V.; Lawac, F.; Michalet, S.; Legendre, L. Characterization of taro [*Colocasia esculenta* (L.) Schott] germplasm for improved flavonoid composition and content. *Plant Genet. Resour.* **2015**, *15*, 260–268. [[CrossRef](#)]
13. Ferreres, F.; Goncalves, R.F.; Gil-Izquierdo, A.; Valentao, V.; Silva, A.M.; Silva, J.B. Further knowledge on the phenolic profile of *Colocasia esculenta* (L.) Shott. *J. Agric Food Chem.* **2012**, *60*, 7005–7015. [[CrossRef](#)]
14. Gupta, K.; Kumar, A.; Tomer, V.; Kumar, V.; Saini, M. Potential of *Colocasia* leaves in human nutrition: Review on nutritional and phytochemical properties. *J. Food Biochem.* **2019**, *43*, e12878. [[CrossRef](#)]
15. Akuz, M. Determination of Antioxidant Activity of Ethanol Extract of Gölevez [(*Colocasia esculenta* (L.)) Tubers. *KSU J. Agric Nat.* **2019**, *22*, 388–394.
16. Liua, H.; Laia, W.; Liua, X.; Yanga, H.; Fanga, Y.; Tiana, L. Exposure to copper oxide nanoparticles triggers oxidative stress and endoplasmic reticulum (ER)-stress induced toxicology and apoptosis in male rat liver and BRL-3A cell. *J. Hazard Mater.* **2021**, *401*, 123349. [[CrossRef](#)]
17. Chea, J.; Lva, H.; Yang, J.; Zhaoa, B.; Zhoue, S.; Yua, T. Iron overload induces apoptosis of osteoblast cells via eliciting ER stress-mediated mitochondrial dysfunction and p-eIF2 $\alpha$ /ATF4/CHOP pathway in vitro. *Cell Signal.* **2021**, *84*, 110024. [[CrossRef](#)]
18. Lin, C.; Lee, C.; Chen, C.; Cheng, C.; Chen, P.; Ying, T. Protodioscin Induces Apoptosis Through ROS-Mediated Endoplasmic Reticulum Stress via the JNK/p38 Activation Pathways in Human Cervical Cancer Cells. *Cell Physiol Biochem.* **2018**, *46*, 322–334. [[CrossRef](#)]
19. Martucciello, S.; Masullo, M.; Cerulli, A.; Piacente, S. Natural Products Targeting ER Stress, and the Functional Link to Mitochondria. *Int. J. Mol. Sci.* **2020**, *21*, 1905. [[CrossRef](#)]
20. Zhu, J.; Xu, S.; Gao, W.; Feng, J.; Zhao, G. Honokiol induces endoplasmic reticulum stress-mediated apoptosis in T human lung cancer cells. *Life Sci.* **2019**, *221*, 204–211. [[CrossRef](#)]
21. Hengstermann, A.; Müller, T. Endoplasmic reticulum stress induced by aqueous extracts of cigarette smoke in 3T3 cells activates the unfolded-protein-response-dependent PERK pathway of cell survival. *Free Radic Biol Med.* **2018**, *44*, 1097–1107. [[CrossRef](#)]
22. Elmore, S. Apoptosis: A review of programmed cell death. *Toxicol Pathol.* **2007**, *35*, 495–516. [[CrossRef](#)]
23. Wei, J.; Liu, R.; Hu, X.; Liang, T.; Zhou, Z.; Huang, Z. MAPK signaling pathway-targeted marine compounds in cancer therapy. *J. Cancer Res. Clin. Oncol.* **2021**, *147*, 3–22. [[CrossRef](#)]
24. Cao, X.; Fu, M.; Bi, R.; Zheng, X.; Fu, B.; Tian, S. Cadmium induced BEAS-2B cells apoptosis and mitochondria damage via MAPK signaling pathway. *Chemosphere* **2021**, *263*, 128346. [[CrossRef](#)] [[PubMed](#)]
25. Darling, N.J.; Cook, S.J. The role of MAPK signalling pathways in the response to endoplasmic reticulum stress. *Biochim. Biophys. Acta* **2014**, *1843*, 2150–2163. [[CrossRef](#)]
26. Yua, J.; Lopez, J. Understanding MAPK Signaling Pathways in Apoptosis. *Int. J. Mol. Sci.* **2020**, *21*, 2346. [[CrossRef](#)]
27. Yangnok, K.; Innajak, S.; Sawasjirakij, R.; Mahabusarakam, W.; Watanapokasin, R. Effects of Artonin E on Cell Growth Inhibition and Apoptosis Induction in Colon Cancer LoVo and HCT116 Cells. *Molecules* **2022**, *27*, 2095. [[CrossRef](#)]
28. Nur-Hadirah, K.; Arifullah, M.; Amaludin, N.A.; Klaiklay, S.; Chumkaew, P.; Zain, N.M. Total phenolic content and antioxidant activity of an edible Aroid, *Colocasia esculenta* (L.) Schott. *IOP Conf Ser Earth Environ Sci.* **2021**, *756*, 012044. [[CrossRef](#)]
29. Gao, X.; Yanan, J.; Santhanam, R.K.; Wang, Y.; Lu, Y.; Zhang, M. Garlic flavonoids alleviate H<sub>2</sub>O<sub>2</sub> induced oxidative damage in L02 cells and induced apoptosis in HepG2 cells by Bcl-2/Caspase pathway. *J. Food Sci.* **2021**, *86*, 366–375. [[CrossRef](#)]
30. Kadar, N.N.; Ahmad, F.; Teoh, S.L.; Yahaya, M.F. Caffeic Acid on Metabolic Syndrome: A Review. *Molecules* **2021**, *26*, 5490. [[CrossRef](#)]
31. Kepa, M.; Miklasińska-Majdanik, M.; Wojtyczka, R.D.; Idzik, D.; Korzeniowski, K.; Smoleń-Dzirba, J. Antimicrobial Potential of Caffeic Acid against *Staphylococcus aureus* Clinical Strains. *BioMed Res. Int.* **2018**, *2018*, 1–9. [[CrossRef](#)] [[PubMed](#)]
32. Espindola, K.M.; Ferreira, R.G.; Mosquera, L.E.; Rosario, A.R.; Silva, A.M.; Silva, A.B. Chemical and Pharmacological Aspects of Caffeic Acid and Its Activity in Hepatocarcinoma. *Front. Oncol.* **2019**, *9*, 1–10. [[CrossRef](#)] [[PubMed](#)]
33. Kilani-Jaziri, S.; Mokdad-Bzeouich, I.; Krifa, M.; Nasr, N.; Ghedira, K.; Chekir-Ghedira, L. Immunomodulatory and cellular anti-oxidant activities of caffeic, ferulic, and p-coumaric phenolic acids: A structure–activity relationship study. *Drug Chem. Toxicol.* **2017**, *40*, 416–424. [[CrossRef](#)] [[PubMed](#)]
34. Prasad, N.R.; Karthikeyan, A.; Karthikeyan, S.; Reddy, B.V. Inhibitory effect of caffeic acid on cancer cell proliferation by oxidative mechanism in human HT-1080 fibrosarcoma cell line. *Mol. Cell Biochem.* **2011**, *439*, 11–19. [[CrossRef](#)]
35. Magnani, C.; Corrêa, M.A.; Isaac, V.; Salgado, H. Caffeic acid: A review of its potential use in medications and cosmetics. *Anal. Methods* **2014**, *6*, 3203. [[CrossRef](#)]
36. Kanimozhi, G.; Prasad, N.R. Anticancer Effect of Caffeic Acid on Human Cervical Cancer Cells. *Coffee Health Dis. Prev.* **2015**, *2015*, 655–661.
37. Smets, L.A. Programmed cell death (apoptosis) and response to anti-cancer drug. *Anticancer Drugs* **1994**, *5*, 3–9. [[CrossRef](#)]
38. Hacker, G. The morphology of apoptosis. *Cell Tissue Res.* **2000**, *301*, 5–17. [[CrossRef](#)]

39. Kim, J.K.; Kang, K.A.; Ryu, Y.S.; Piao, M.J.; Han, X.; Oh, M.C. Induction of Endoplasmic Reticulum Stress via Reactive Oxygen Species Mediated by Luteolin in Melanoma. *Anticancer Res.* **2016**, *36*, 2281–2289.
40. Chiun, T.; Su, C.C. Tanshinone IIA increases protein expression levels of PERK, ATF6, IRE1 $\alpha$ , CHOP, caspase-3 and caspase-12 in pancreatic cancer BxPC-3 cell-derived xenograft tumors. *Mol. Med. Rep.* **2017**, *15*, 3259–3263.
41. Wang, X.; Zhuang, Y.; Fang, Y.; Cao, H.; Zhang, C.; Xing, C. Endoplasmic reticulum stress aggravates copper-induced apoptosis via the PERK/ATF4/CHOP signaling pathway in duck renal tubular epithelial cells. *Environ. Pollut.* **2020**, *272*, 115981. [[CrossRef](#)]
42. Li, X.; Wang, D.; Sui, C.; Meng, F.; Sun, S.; Zheng, J. Oleandrin induces apoptosis via activating endoplasmic reticulum stress in breast cancer cells. *Biomed. Pharmacother.* **2020**, *124*, 109852. [[CrossRef](#)]
43. Kamiya, T.; Nishihara, H.; Hara, H.; Adachi, T. Ethanol Extract of Brazilian Red Propolis Induces Apoptosis in Human Breast Cancer MCF-7 Cells through Endoplasmic Reticulum Stress. *J. Agric. Food Chem.* **2012**, *60*, 11065–11070. [[CrossRef](#)]
44. Kadam, C.Y.; Abhang, S.A. Apoptosis Markers in Breast Cancer Therapy. *Adv. Clin. Chem.* **2016**, *74*, 143–193.
45. Lamkanfi, M.; Kanneganti, T. Caspase-7: A protease involved in apoptosis and inflammation. *Int. J. Biochem Cell Biol.* **2012**, *42*, 21–24. [[CrossRef](#)]
46. Gee, M.M.; Hyland, E.; Campiani, G.; Ramunno, A.; Nacci, V.; Zisterer, D.M. Caspase-3 is not essential for DNA fragmentation in MCF-7 cells during apoptosis induced by the pyrrolo-1,5-benzoxazepine, PBOX-6. *FEBS Lett.* **2002**, *515*, 66–70.
47. Chang, W.; Hsieh, C.; Hsiao, M.; Li, W.; Hung, Y.; Ye, J. Caffeic acid induces apoptosis in human cervical cancer cells through the mitochondrial pathway. *Taiwan J. Obstet. Gynecol.* **2010**, *49*, 419–424. [[CrossRef](#)]
48. Tseng, T.; Shen, C.; Huang, W.; Chen, C.; Liang, W.; Lin, T.; Kuo, H. Activation of neutral-sphingomyelinase, MAPKs, and p75 NTR-mediated caffeic acid phenethyl ester-induced apoptosis in C6 glioma cells. *J. Biomed. Sci.* **2014**, *21*, 61. [[CrossRef](#)]
49. Inoshita, S.; Takeda, K.; Hatai, T.; Terada, Y.; Sano, M.; Hata, J. Phosphorylation and inactivation of myeloid cell leukemia 1 by JNK in response to oxidative stress. *J. Biol. Chem.* **2002**, *277*, 43730–43734. [[CrossRef](#)]
50. Yamamoto, K.; Ichijo, H.; Korsmeyer, S.J. BCL-2 is phosphorylated and inactivated by an ASK1/Jun N-terminal protein kinase pathway normally activated at G(2)/M. *Mol. Cell Biol.* **1999**, *19*, 8469–8478. [[CrossRef](#)]
51. Cai, B.; Chang, S.H.; Becker, E.B.; Bonni, A.; Xia, Z. p38 MAP Kinase Mediates Apoptosis through Phosphorylation of BimEL at Ser-65. *J. Biol. Chem.* **2006**, *281*, 25215–25222. [[CrossRef](#)]
52. Hiraishi, N.; Kanmura, S.; Oda, K.; Arima, S.; Kumagai, K.; Mawatari, S. Extract of *Lactobacillus plantarum* strain 06CC2 induces JNK/p38 MAPK T pathway-mediated apoptosis through endoplasmic reticulum stress in Caco2 colorectal cancer cells. *Biochem. Biophys. Rep.* **2019**, *20*, 100691. [[CrossRef](#)]
53. Srivastava, R.K.; Mi, Q.; Hardwick, J.M.; Longo, D.L. Deletion of the loop region of Bcl-2 completely blocks paclitaxel-induced apoptosis. *Proc. Natl. Acad. Sci. USA* **1999**, *96*, 3775–3780. [[CrossRef](#)]
54. Yao, Z.; Sun, B.; Hong, Q.; Yan, J.; Mu, D.; Li, J.; Sheng, H.; Guo, H. Pace4 regulates apoptosis in human prostate cancer cells via endoplasmic reticulum stress and mitochondrial signaling pathways. *Drug Des. Devel. Ther.* **2015**, *9*, 5911–5923.
55. Lei, K.; Davis, R.J. JNK phosphorylation of Bim-related members of the Bcl2 family induces Bax-dependent apoptosis. *Proc Natl. Acad. Sci. USA* **2003**, *100*, 2432–2437. [[CrossRef](#)]